The Effect of Agricultural Development on Streamflow

Alireza Borhani Dariane (borhani@kntu.ac.ir)
K.N. Toosi University of Technology https://orcid.org/0000-0002-8540-9870
Sepehr Farhoodi
K N Toosi University of Technology

Research Article

Keywords: Land-Use Change, ENVI, SWAT, SWAT-CUP, Irrigated Agriculture, Urmia Lake

Posted Date: May 10th, 2021

DOI: https://doi.org/10.21203/rs.3.rs-304679/v1

Abstract

In recent decades, the amount of water in Urmia Lake has faced a considerable decrease. Several studies evaluated agricultural development as one of the main governing factors. The current study investigates the effect of agricultural development on the amount of streamflow in one of the main Urmia Lake sub-basins. To focus on agricultural development, a novel method using DEM and NDVI information was utilized to distinguish the agriculture class for selected years. Outputs of SWAT model for different years and scenarios revealed that agricultural development from the year 1977 to 2015, increased the annual evapotranspiration from 295 to 308 mm, and decreased the annual streamflow from 317 mcm to 300 mcm for the irrigation scenario. In addition, the groundwater level fluctuations captured by the SWAT, showed 1.9 meters drawdown in the Sarab plain from the year 1992 to 2003, which was in accordance with the observed trend during this period.

1. Introduction

In recent decades, the amount of water in the Urmia Lake faced a considerable decrease. Several studies evaluated different parameters responsible for this issue, including climate change, constructing dams on the main feeding rivers, and increasing cultivated areas (Eamen and Dariane, 2014; Fathian et al., 2016; Schulz et al., 2020). In this research, we assess the effect of land-use change on the amount of streamflow in Merkid hydrometric station located in Ajichai basin, which is one of the main Urmia Lake sub-basins. In addition, we investigate its impact on groundwater fluctuations and its interaction with streamflow.

Monitoring land-use change in time using different satellite images is one of the most well-known applications of remote sensing in studying water resources systems. For instance, Xiao et al. (2006) applied the geographical information system (GIS) and remote sensing to evaluate the temporal and spatial characteristics of urban expansion. Zurqani et al. (2018) studied land-use change in the Savannah river basin using Google Earth Engine, and concluded that the most changes were as a result of deforestation and reforestation in the area. Abd El-Kawy et al. (2011) studied the land-use change in the western Nile region using 4 Landsat images for the years 1984, 1999, 2005, and 2009. For further accuracy, they employed post-classification methods such as visual interpretation and image enhancement. They concluded that the most evident land-use changes are the conversion of barren land into agricultural land. In order to study the impact of land-use change on the amount of streamflow, Quyen et al. (2014) compared water discharges and total water yields for the reference year (2000) and the year 2010. Results did not show a considerable difference between water discharges since the land-use did not change massively. Gashaw et al. (2018) assessed the effect of land-use changes, and land cover change on the Ecosystem Service Value. In their study, the Hybrid land-use classification technique and the Cellular Automata Markov (CA-Markov) were used for classifying Satellite images and land-use/cover forecasting, respectively. In another study, Schilling and Libra (2003) considered the effect of changes in agricultural fields, surface slope, and soil permeability on baseflow contribution to streamflow in different parts of Iowa state, and concluded that increasing agricultural fields resulted in baseflow

increase over the surface runoff. As another example of application of remote sensing in water-related studies, Thanapakpawin et al. (2007) applied DHSVM hydrological model to evaluate the effect of land-use change on the hydrological regime for irrigation and no-irrigation scenarios in the Mae Chaem basin located in the North-West of Thailand. It was concluded that in the irrigation scenario, changes from forest land into agricultural land decreased basin discharge, whereas in the no-irrigation scenario, changes from forest land into agricultural land increased basin discharge.

For Satellite image classification, several digital change detection techniques, namely univariate image differencing, image regression, image rationing, vegetation index differencing, principal components analysis, post-classification comparison, direct multi-data classification, change vector analysis, and background subtraction, have been developed (Singh, 1989). On the other hand, the standard deviation threshold, supervised and unsupervised analysis techniques, as shown by Nelson (1983), are among the most well-known techniques that have been frequently used to classify images. Among the aforementioned digital change detection techniques, univariate image differencing techniques was determined as the most accurate method (Singh, 1989).

The main satellite imagery projects frequently used in remote sensing studies are Spot, NOAA, MODIS, IKONOS, QuickBird, and Landsat. The basic advantage of Landsat imagery for change detection studies, among the others, is its long temporal coverage, which makes it the most suitable imagery product for the change detection studies (Xie et al., 2008). Besides, multispectral remote sensing is capable of capturing reflected radiation in the visible and near-infrared regions in which the most vegetation radiative changes occur (Muttitanon and Tripathi, 2005). The Landsat imagery covers a broad historical timeline since 1972. In this time period, Landsat imagery has been continuously providing scientists with accurate multispectral images that cover all parts of Earth. Furthermore, the capabilities of Landsat imagery have been enhancing in time by adopting more sophisticated sensors. The Landsat 1 to 3, covered the duration of 1972–1983 years, were equipped with Multispectral Scanner (MSS). The more advanced sensor was loaded on satellite 4 and 5 named Thematic Mapper (TM), which provides images with a spatial resolution of 30 meters. Landsat 6 was equipped with the next-generation sensor named Enhanced Thematic Mapper (ETM). However, it did not achieve orbit and went out of service. The Landsat 7 was launched in 1999, loading Enhanced Thematic Mapper Plus (ETM+) sensor armed with a panchromatic band with 15m spatial resolution. However, the project was unsuccessful due to the Scan Line Corrector (SLC) problem resulted in non-accurate imagery. The most recent Landsat product is Landsat 8, which has been in operation since 2013 and provides the most accurate Landsat images by taking advantage of its two instruments, namely the Operational Land Imager (OLI) and the Thermal Infrared Sensors (TIRS), which are able to provide seasonal images with the spatial resolution of 30 meters that can be improved to 15 meters using its panchromatic sensor (https://landat.gsfc.nasa.gov/). Numerous research have recently employed different Landsat imagery products to detect land-use and land cover changes in different parts of the world (Coulter et al., 2016; Devolent et al., 2017; Islam et al., 2018). Nevertheless, it is worth bearing in mind that the digital change detection techniques classify images solely based on the reflected radiation, and as a result, it cannot distinguish between different classes with the same spectral characteristics. This disadvantage becomes noticeable, more specifically, in

studies with the focus on the irrigation practices, in which agricultural fields need to be differentiated from rangeland fields. In this paper, a novel post-classification method using the NDVI (Normalized Difference Vegetation Index) and DEM (Digital Elevation Model) has been applied to images derived from Landsat 5 to reclassify vegetation class into agriculture and rangeland classes.

In order to quantify the land-use change effects on hydrology, different hydrological models have been utilized by different researchers, including PRMS (Leavesley et al., 1984), DHSVM (Wigmosta et al., 1994), and SWAT (Arnald et al., 1998). SWAT is a physically-based semi-distributed hydrological model developed to carry out basin-scale simulations. SWAT model can be used in watersheds without sufficient or well-organized data (Arnald et al., 1998). The model is executable on a daily, monthly, or annual basis. For simulation, the whole watershed is divided into several Hydrologic Response Units (HRUs) based on the soil classes, land-use classes, and slope characteristics.

The model efficacy in studying the effects of land-use changes on streamflow has been widely investigated and proven (e.g., Du et al., 2013; Fohrer et al., 2001; Ghaffari et al., 2010). However, the effect of land-use changes, which is likely to be followed by changes in management practices, more specifically in semi-arid regions, on both groundwater and surface flow has been rarely analyzed. Since the growth in agricultural fields and subsequent irrigation practices have been highlighted as the main factors that resulted in a decrease in both Urmia Lake area and level in several studies (Dariane and Eamen, 2017; Eamen and Alireza B. Dariane, 2014; Eimanifar and Mohebbi, 2007; Hassanzadeh et al., 2012), the effect of land-use change on irrigation practices from both surface and ground reservoirs must be taken into account. Different pieces of research have made efforts to solve groundwater equations in the SWAT model. The most famous method in this regard has been the use of MODFLOW to solve the groundwater flow equations and the SWAT for handling the surface flow equations (Dowlatabadi and Zomorodian, 2016; Kim et al., 2008). This approach was later developed as a coupled SWAT-MODFLOW model (Bailey et al., 2016). Although the coupled SWAT-MODFLOW model has some advantages, including geographically located HRUs and effective HRU mapping procedure between two models, but it also has a substantial drawback of not calibrating both models simultaneously. Accordingly, relying solely on the integrated SWAT hydrological model for both groundwater and surface water fluctuations has been suggested (Ahmadzadeh et al., 2016). Furthermore, SWAT model has shown its capability of assessing the management procedures on the hydrologic responses in terms of groundwater and surface water alterations (Baker and Miller, 2013).

The main objective of this paper is to study the land-use change effects on the amount of streamflow in Ajichai basin. In order to fulfill this objective, different land-use maps were generated using satellite data. Afterward, SWAT model was calibrated and validated for one of the land-use maps and then executed for the other generated land-use maps. In order to accurately simulate hydrological processes within the basin, we applied the irrigation practices to the basin with the help of the study area’s aquifer map and water usage reports provided by the energy ministry of Iran. In addition, we aimed to compare groundwater drawdown simulated by SWAT with the observed values to show SWAT capability in simulating groundwater drawdown if irrigation data is accurately imported to the model.

2. Study Area And Data

2.1 Study Area

The case study is Ajichai basin above Merkid hydrometric station (Fig. 1). Ajichai located in East Azerbaijan, Iran, is one of the biggest sub-basins in Urmia Lake and has a pivotal role in feeding the Lake, mainly through early spring floods and snowmelts. The basin is situated between 46º 33´ and 47º 54´ eastern longitudes and 37º 36´ and 38º 24´ northern latitudes. The basin area and length of main river branch above Merkid are 5460 km^2 and 111 km, respectively.

2.2 Data

The climatic variables needed for executing the SWAT model are daily precipitation, daily minimum and maximum temperature, solar radiation, wind speed, and relative humidity. Nevertheless, the SWAT model is executable, relying solely on daily minimum and maximum temperature as well as the daily precipitation. In this study, six precipitation stations and two temperature stations were chosen as data stations. These stations were selected according to their data availability and proper distribution within the case study area. Figure 1 and Table 1 respectively show the dispersion of the stations and information regarding each station.

The elevation of the basin ranges between 1503 to 3724 meters above sea level (Fig. 1) and is captured using DEM data obtained from the Advanced Spaceborne Thermal Emission and Reflection Radiometer (ASTER) Global Digital Elevation Model Version 3 (GDEM 003) which is jointly released by The Ministry of Economy, Trade, and Industry (METI) of Japan and the United States National Aeronautics and Space Administration (NASA) (https://asterweb.jpl.nasa.gov/gdem.asp). The spatial resolution of the product is 30 meters. Soil characteristics of the case study have been acquired from FAO (Food and Agriculture Organization of the United Nations) (http://www.fao.org). The soil map is divided into five predefined classes (Fig. 2). In Fig. 2, gray, and green colors represent loam soil texture, while the other colors represent clay-loam soil texture. Readers are referred to FAO website for further detailed information about each class's characteristics (http://www.fao.org).

Table 1
Hydro-meteorological stations located within the case study

Station name	Gauging station type	Longitude	Latitude	Height (m)	Data span
Sahzab	Precipitation	47.67	37.97	1850	1974–2016
Sarab	Precipitation	47.53	37.95	1800	1966–2016
Doozdoozan	Precipitation	47.12	37.95	1655	1979–2016
Bostanabad	Precipitation	46.83	37.85	1750	1972–2016
Heris	Precipitation	47.12	38.25	1962	1976–2016
Asbkhoran	Precipitation	46.97	38.33	1940	1980–2016
Sarab	Temperature	47.53	37.93	1682	1980–2016
Tabriz	Temperature	46.28	38.08	1361	1951–2016
Merkid	Hydrometric	46.82	38.17	1518	1992–2016

3. Methods

3.1 Land-use maps generation

In this study, we downloaded Landsat MSS satellite images for the year 1977, Landsat TM images for the years 1993 and 2005, and Landsat OLI images for the year 2015 from the Earth Explorer extension of the United States Geological Survey (USGS) website (https://earthexplorer.usgs.gov/). It should be noted that three satellite images (three different paths and rows according to the USGS website) were obtained for each year due to extensive coverage of the case study. Afterward, the satellite images were processed to generate land-use maps for the selected years. The land-use map generation procedure using the obtained satellite images is discussed in the following sections.

3.1.1 Images classification

In order to classify images, Environment software for Visualizing Images (ENVI) was used. It has been concluded that the pre-classification process is necessary for a classifying scheme (Coppin et al., 2004). In this study, image enhancement techniques that are available in ENVI software were utilized to enhance the visual quality of images. Pre-classification steps, such as radiometric and atmospheric correction, were applied in advance to prepare images for classification. Overall, classification methods are categorized into two main groups, namely unsupervised and supervised. In unsupervised method, pixels are divided into separated clusters based on their reflectance characteristics. K-means and ISO (Iterative Self Organizing) are examples of widely used algorithms in this regard. On the other hand, in the supervised classification method, classification is carried out based on samples that are attributed to each class by the user. Mostly used supervised classification algorithms are Maximum Likelihood,

Minimum Distance, and Artificial Neural Network (ANN). In this study, the ANN algorithm was employed to classify the images into four classes, namely residential, water, soil-pasture, and vegetation. To do so, samples were selected by drawing polygons representing each class. Representative polygons for each class are defined as ROI (Region of Interest) in the ENVI software. It should be noted that for classification results to be beneficial for change detection studies, classification accuracy should be evaluated initially (Owojori and Xie, 2005). Accordingly, to validate the accuracy of the classification method, 200 well-distributed points in each image were taken into account as the ground truth data. The confusion error matrix in the ENVI software was employed to make a comparison between classification results and ground truth data. As said before, we had to use three images for each year due to the huge coverage of our study area. Thus, the abovementioned steps proceeded for every three images related to each year. Afterward, mosaic tools in ArcGIS software were used to merge images for each year.

3.1.2 Splitting vegetation class into agriculture and rangeland

As discussed before, the increase in agricultural fields and subsequent irrigation practices have been considered as one of the main factors resulting in a decrease in the Urmia Lake area and level. Therefore, we needed to separate the agriculture class from the vegetation class to detect where irrigation practices should be applied. To fulfill this purpose, we employed a novel technique for splitting the vegetation class into agriculture and rangeland classes. In this technique, the DEM image and NDVI index are used simultaneously to distinguish agriculture class from rangeland class.

NDVI is a well-known index for detecting vegetation (Lunetta et al., 2006). Besides, the NDVI index is also able to differentiate between the agricultural fields and rangeland fields in a region as it is related to the vegetation density. Generally, NDVI values between 0 to 0.1, 0.2 to 0.3, and 0.3 to 1 are in accordance with barren, rangeland, and denser vegetation fields, respectively (Gross, 2005). Additionally, DEM images can be used for splitting agricultural fields from rangeland fields since DEM images represent topographic information that can be related to vegetation characteristics (Moore et al., 1991). Meanwhile, we expect rangeland fields to be located at higher elevations than agricultural fields. Therefore, the DEM image was used to specify an elevation threshold to stand for various elevations that are expected for agricultural and rangeland fields. In order to use both NDVI and DEM information to finer classify the vegetation class, a decision tree process was developed using ENVI software. In this regard, it was necessary to firstly produce NDVI images. To do so, we initially rescaled pixels values of our multispectral satellite images to lie between 0 and 1. Afterward, NDVI values were computed for each image by applying the NDVI equation using the Band math tool in the ENVI software. In Fig. 3 the resulted NDVI image is shown.

In order to apply our decision tree, two-band combined NDVI-DEM images were required. As a result, the DEM image was merged with the generated NDVI image. Having two-band combined NDVI-DEM images, the threshold value of 0.3, as suggested by (Gross, 2005), was applied on the NDVI band to separate the agriculture fields from the other classes. Subsequently, to further exclude the agriculture fields from the

rangeland fields, the elevation threshold was used on the DEM image. An intuitive scheme of the decision tree discussed above is demonstrated in Fig. 4.

After splitting the vegetation class into agriculture and rangeland classes, ArcMap software was used again to eventually produce land-use maps for each year containing five classes, namely residential, water, soil-pasture, agriculture, and rangeland.

3.2 Hydrologic Modelling using SWAT model

As mentioned earlier, in order to evaluate how different land-use practices affect river discharge, we used SWAT hydrologic model. SWAT is a physically-based hydrological model that is able to simulate different hydrological processes, including streamflow. The model uses general hydrological equations to simulate streamflow and the other hydrologic outputs. SWAT is a continuous-time model and is capable of simulating hydrological processes on a daily, monthly, or annual time scale. SWAT divides each basin to finer sub-basins, and each sub-basin to several HRUs based on similar land-use, soil, and slope characteristics. For simulation, the amount of water stored in the soil, streamflow, nutrient cycle, sediment, plant growth, and management practices are initially calculated for each HRU, and subsequently computed for each sub-basin using a weighted average. SWAT requires different inputs to proceed, including DEM, location of hydrometric stations, rainfall and temperature data, soil and land-use map, and management data (Arnald et al., 1998).

3.2.1 Model setup

In this study, ArcSWAT interface for SWAT2012 was utilized for the simulation processes. To set up the model for our case study, SWAT requires different inputs, ranging from land-use map, soil map, DEM, climate inputs, and management information. Depending on the study's purpose, the management information can be imported into the model or can be neglected. SWAT has shown its robustness in taking into account the management practices (Neitsch et al., 2011). Furthermore, as noted before, since this study's main focus is to consider the probable effect of the management operations on the amount of streamflow, management information needs to be involved.

In practice, the basin was delineated using ArcSWAT interface. The interface carries out this process automatically by importing the DEM, drainage area, and the location of the hydrometric station at the outlet of the basin. Afterward, the generated land-use map and soil map derived from the FAO were imported to stand for the HRUs characteristics. In addition, the agriculture class is further divided into the main crops of the study area, which are spring wheat, spring barley, green beans, alfalfa, potato, tomato, and apple. Consequently, a total of 44 sub-basins and 556 HRUs were delineated. Precipitation data for six rainfall gauging stations were obtained from the Iran Water Resources Management Organization, and temperature (minimum and maximum) and two synoptic stations were obtained from the Iran Meteorological Organization.

3.2.2 Irrigation

Since one of the main objectives of the current study is to tackle land-use change and the resulted irrigation practice changes on the amount of streamflow, data and statistics have been assessed to provide insights into the cultivation patterns and the irrigation sources.

We used data from the National Water Document of Iran (NWDI) to gain information concerning the cultivation pattern for our case study. This document, for a various number of basins in Iran, represents planting and harvesting date for the main crops.

Another required irrigation data is the source of irrigation that can be specified in SWAT model as reach, shallow aquifer, deep aquifer, reservoir, or unlimited source outside basin (Neitsch et al., 2011). To determine the irrigation source for each sub-basin, we used the report on water master plan studies for Urmia Lake developed by the ministry of energy of Iran. Based on this report, reach and aquifer were detected as two primary sources of irrigation for the study area. In addition, on a sub-divided map, the utilization percentage of each of these primary irrigation sources has been determined. We used this map and its utilization percentage information to determine irrigation sources for our sub-basins. Moreover, in order to better assign irrigation sources, we matched the basin's aquifer map with the modeled basin to detect which sub-basins are more likely to be fed from the aquifer (Fig. 5). By analyzing data and maps mentioned above, we allocated the irrigation source codes to each sub-basin.

3.3 Calibration and Validation

3.3.1 Sensitive parameters

In this study, we used SWAT-CUP software (Abbaspour et al., 2007b) and its Sequential Uncertainty Fitting version 2 (SUFI-2) (Abbaspour et al., 2004) algorithm for calibration and validation processes. The other calibration algorithms in this software include Particle Swarm Optimization (PSO) (Kennedy and Eberhart, 1995), Generalized Likelihood Uncertainty Estimation (GLUE) (Beven and Binley, 1992), Parameter Solution (ParaSol) (van Griensven and Meixner, 2006), and Markov Chain Monte Carlo (MCMC) (Kuczera and Parent, 1998). SWAT model was executed for the 1993 land-use map on the monthly time scale and then SWAT-CUP software was used to test streamflow outputs against monthly discharge observations of the Merkid hydrometric station from the year 1989 to 2003. The outputs for the first three years were neglected to account for the warm-up period. The calibration process in SWAT needs certain steps to be taken which is explained as follows.

In this software, the calibration and validation processes need to start with selecting the sensitive parameters to the streamflow. Furthermore, the changing range of each parameter, and the type of change to be applied to the parameters should be determined. SWAT is equipped with three different types of sampling methods to replace parameter values with the new ones within each parameter's changing range. These are relative change, replace, and absolute methods. In the relative change method, the parameter value of each HRU is replaced by a fraction of its initial value after each iteration. In the replace method, the new values of each parameter replace the former values for all HRUs. Finally, in the

absolute method, a given value is added to the former parameter value, and the new value replaces the parameter value for all HRUs.

It should be noted that for spatial parameters such as curve number (CN2), the relative change method is suggested as these parameters should be set independently from one HRU to another (Abbaspour et al., 2007a). Moreover, it is also important to know that the changing range of some parameters is limited to a predetermined range and cannot exceed that range. For instance, CN2 value is closely correlated with soil and land-use maps that are inputs to the model. As a result, by changing the CN2 values by more than 20 percent, the inputs, in this case, soil and land-use maps information will also change. According to the above-mentioned explanations, the sensitive parameters to the streamflow, their sampling method and their changing range were chosen as shown in Table 2.

Table 2
Sensitive parameters along with their exploration method and min and max values

Parameter	Min. value	Max. value	Description
r__CN2.mgt	-0.2	0.2	SCS runoff curve number for moisture condition II
r__SOL_AWC().sol	-0.5	0.5	Available water capacity of the soil layer
v__GWQMN.gw	100	3000	Threshold depth of water in the shallow aquifer required for return flow to occur (mm H2O).
v__GW_DELAY.gw	1	60	Groundwater delay time (days)
v__ALPHA_BF.gw	0	1	Base flow alpha factor (days)
v__ESCO.hru	0.01	1	Soil evaporation compensation factor
r__SOL_K().sol	-0.8	0.8	Saturated hydraulic conductivity y
r__SOL_BD().sol	-0.5	0.5	Moist bulk density (Mg/m3 or g/cm3)
v__SMFMN.bsn	1	7	Melt factor for snow on December 21 (mm H2O/°C-day)
v__GW_REVAP.gw	0.02	0.2	Groundwater "revap" coefficient
v__CH_K(2).rte	0.1	1000	Effective hydraulic conductivity in main channel alluvium (mm/hr)
v__ALPHA_BNK.rte	0	1	Baseflow alpha factor for bank storage (days)
v__CANMX.hru	0	100	Maximum canopy storage (mm H2O)
v__SMFMX.bsn	1	7	Melt factor for snow on June 21 (mm H2O/°C-day)
v__SURLAG.bsn	1	24	Surface runoff lag coefficient
v__TIMP.bsn	0.01	1	Snowpack temperature lag factor
v__SMTMP.bsn	0	3	Snow melt base temperature (°C)

3.3.2 Different parameterization schemes

In order to optimize the calibration and validation processes, two schemes were considered in the parameterization process, which is described below.

Modifying or not modifying the changing range after each set of iterations

As explained in the SWAT-CUP manual, the changing range of parameters is updated after each set of iterations. Nonetheless, in many cases, the suggested range for the next set of iterations exceeds the model's acceptable range for the parameter. In these cases, it was suggested to manually modify the suggested range to the acceptable range in order to optimize the calibration process (Abbaspour et al., 2007b). However, in this study, we also explored not modifying the suggested range for the next set of iterations. The reason is that in case of unacceptable values, SWAT replaces the unacceptable values by either the maximum or minimum value of that parameter. By not limiting the proposed range, we explored new combinations of parameters values. Since the parameterization is a collaborative process, this exploring procedure might produce more favorable outcomes.

Choosing the objective function

Changing range proposed by the SWAT-CUP for the next set of iterations also depends on the selected objective function for the optimization. We explored R^2 and Nash-Sutcliffe Efficiency Index (NS) as two different objective functions in this study.

By applying different parameterization schemes mentioned above, the changing range modification, and NS as the objective function generated better results.

4. Results And Discussions

4.1 Generated land-use maps

Based on the explanations brought in Sect. 3.1, the land-use maps were generated for the years 1977, 1993, 2005, and 2005. Each land-use map was classified into 5 classes, namely water, residential, soil-pasture, agriculture, and rangeland (Fig. 6).

4.2 Changing trend of agriculture and residential areas

The agriculture and residential areas of each image were computed using the aforementioned maps for the selected years (Fig. 7a). After calculating the agricultural and residential land areas for each year, the change percentage of each class was computed as shown in Fig. 7b.

According to Figs. 7, although agricultural land expansion is viewed in all the selected years, in some periods, the expansion trend is steeper. According to Fig. 7a, agricultural land area for years 1977, 1993, 2005, and 2015 is 218, 313, 799, and 896 km^2, respectively. Moreover, according to Fig. 7b, the

agricultural land area faced 44%, 267%, and 312% increase from the year 1977 to the years 1993, 2005, and 2015 respectively. As it can be seen from Fig. 7b, the agricultural land did not grow remarkably from the year 1977 to the year 1993 due to the Iran-Iraq war that began in 1980 and ended in 1988. The war resulted in a slight increase and in some cases a decrease in agricultural land area in different parts of Iran. As opposed to this period, the agricultural land area surged up from the year 1993 to 2005. Generally speaking, a part of this increase can be related to the population growth in this time period, and accordingly, increase in need for agriculture, however the government policy toward self-sufficiency in important goods such as wheat is the main reason behind this sharp increase. The same policy has caused devastating impacts on water scarcity in the area and Urmia Lake drying up crises.

Furthermore, other factors, such as desirable weather conditions, lack of proper careers in different fields, and the availability of agricultural facilities in this time period also caused an increase in agricultural land. During this period, the governmental policies in Iran toward self-sufficiency caused a 155% expansion in agricultural land area. As the drought period began between the years 2005 and 2015, the agricultural land growing trend, once more, faced a decrease as a consequence of precipitation decrease, the decline in groundwater level, and other obstacles that farmers faced at that time.

In the study area, as seen in Fig. 7a, the residential area has always increased as analogous to the other regions of Iran. According to Fig. 7a, the residential area was around 3 km^2 in the year 1977 and increased to 9, 21, and 44 $km^2$for the years 1993, 2005, and 2015 respectively. Additionally, as shown by Fig. 7b, the change percentage of the residential area from the year 1977 to the years 1993, 2005, and 2015 are 196%, 635%, and 1454%, respectively.

4.3 Calibration and Validation

After generating the land-use maps for the proposed years (i.e. 1977, 1993, 2005, and 2015), the 1993 land-use map was taken as the primary map for proceeding the calibration and validation steps. Therefore, the model was initially run for the 1993 land-use map on monthly time scale and then calibrated against monthly discharge observations of the Merkid hydrometric station from the year 1992 to 1999, and later, validated for the year 2000 to 2003. Figure 8 shows the monthly average of the simulated and observed streamflow for both the calibration and validation periods. Furthermore, the R^2 and NS values for the calibration and validation periods were found to be 0.74, 0.73 and 0.74, 0.64 respectively.

Next, to evaluate the effect of land-use change on the amount of streamflow for other years, the 1993 land-use map was replaced by 1977, 2005, and 2015 land-use maps and the calibrated model was executed again. Advantage of this approach to study the effect of land-use change on the amount of streamflow is that the land-use map is the only variable in different model runs. In contrast, in some other land-use change effect studies, the land-use update option in the SWAT model is used to stand for the land-use changes in time. However, in those approaches, the variation of other climatic variables, and more specifically rainfall, also take parts and are responsible for the streamflow changes. Therefore, the changes in the simulated streamflow cannot be solely related to the changes in land-use.

4.4 Comparing the simulated and observed groundwater level

As explained in Sect. 3.2.2, the aquifer map of the study area was utilized to more accurately assign the groundwater irrigation source to each sub-basin. In order to show the capability of the SWAT model in simulating the amount of water derived from groundwater source in each sub-basin, accumulated groundwater drawdown simulated by SWAT for the Sarab plain, one of the central plains of the study area, was compared with the observation values from 1992 to 2003 (Fig. 9).

According to Fig. 9, SWAT proves its ability to capture the groundwater drawdown trend. However, in some years, a noticeable gap is evident between the simulated and observed values. This gap is mainly as a result of not calibrating the simulated groundwater drawdown against the observed values, noting that the streamflow calibration was the priority of this research. Nevertheless, the calibration of the simulated groundwater drawdown against the observation values is suggested for future studies.

4.5 Simulation results for 1977, 2005, and 2015 land-use maps

As it was mentioned in Sect. 4.3, after achieving reasonable results for the calibration and validation periods for the 1993 land-use map model, this map was replaced by the land-use maps for the years 1977, 2005, and 2015 and the model was run for each case based on the calibrated parameters obtained for the 1993 land-use map. It should be noted that since by changing the land-use map, the area of each land-use class, and accordingly, the number of HRUs alter, it was necessary to apply the irrigation practices for each land-use map again. The number of sub-basins for all years stayed the same at 44 levels. However, the number of HRUs for 1977, 1993, 2005, and 2015 were respectively determined as 556, 610, 614, and 587. The average annual ET and streamflow for the selected years are shown in Fig. 10a. According to this Figure, the amount of ET increased from 295 mm in year 1977 to 308 mm in year 2015. Consequently, the amount of streamflow decreased from 317 mcm in year 1977 to 300 mcm in year 2015.

In order to also address the effect of irrigation practices on these changes, the model was run, once more without applying the irrigation practices for the years 1977, 1993, 2005, and 2015. The results are presented in Fig. 10b.

According to Fig. 10b, the ET values increased from 293.5 mm in year 1977 to 300 mm in year 2015. Consequently, the amount of streamflow decreased from 323 mcm in year 1977 to 314 mcm in year 2015.

To reveal how each scenario affects the ET and streamflow values from the year 1977 to the year 2015, the changes in these values are represented and compared in Figs. 11.

According to Fig. 11a, for both scenarios, ET increased in all simulated years as a result of an increase in the agricultural land. However, the ET values are higher for the irrigation scenario than the no-irrigation scenario due to the fact that irrigation practices make more water accessible for evapotranspiration. Additionally, as a reflection on the increase in ET, the streamflow values declined in time for both scenarios. However, this decrease is more evident for the irrigation scenario due to more water consumption, both from surface and groundwater sources (Fig. 11b).

5. Conclusions

The main objective of this study was to investigate the effect of land-use change (i.e., agricultural development) on the amount of streamflow considering surface-groundwater interactions. To do so, we initially produced land-use maps for the years 1977, 1993, 2005, and 2015, including water, residential, soil-pasture, and vegetation classes. Afterward, using a novel approach we further classified the vegetation class into agriculture and rangeland classes to apply the management practices only to the agriculture class. We concluded that the agricultural land areas have continuously increased during the years considered in a way that the agricultural land areas faced a 312% increase from the year 1977 to the year 2015.

In the second part of the current study, in order to see how this increase in agricultural land affected the ET and streamflow values, we, firstly, set up and calibrated the SWAT model for the 1993 land-use map, and eventually, ran the model for the other land-use maps individually using two scenarios of irrigation and no-irrigation for agricultural areas. Results indicated that the amount of ET increased and the amount streamflow decreased in both scenarios from the year 1977 to the year 2015 due to agricultural developments in the basin. Nonetheless, the increase in the ET values and the decrease in the streamflow values were more evident in the irrigation scenarios due to more water consumption, both from surface and groundwater sources. According to the results obtained in this research, the agricultural development could be partially responsible for the Lake Urmia desiccation.

Declarations

Declaration of competing interest

The authors declare that they have no known competing financial interests or personal relationships that could have appeared to influence the work reported in this paper.

Contributions

Both authors contributed to the study in all levels and original draft preparation. The study is the result of a graduate level thesis and was guided by Alireza Borhani Dariane as the advisor of Sepehr Farhoodi (student).

Funding

No funding was used in this research.

Availability of data and materials

All authors made sure that all data and materials support our published claims and comply with field standards.

References

1. Abbaspour, K. C., Johnson, C. A. and Genuchten, M. T. van., 2004. Estimating Uncertain Flow and Transport Parameters Using a Sequential Uncertainty Fitting Procedure, Vadose Zone Journal, 3(4), 1340–1352. https://doi.org/10.2136/vzj2004.1340.
2. Abbaspour, K. C., Yang, J., Maximov, I., Siber, R., Bogner, K., Mieleitner, J., Zobrist, J. and Srinivasan, R., 2007a. Modelling hydrology and water quality in the pre-alpine/alpine Thur watershed using SWAT, Journal of Hydrology, 333(2–4), 413–430. https://doi.org/10.1016/j.jhydrol.2006.09.014.
3. Abbaspour, K. C., Vejdani, M., Haghighat, S. and Yang, J., 2007b. SWAT-CUP calibration and uncertainty programs for SWAT, MODSIM 2007 International Congress on Modelling and Simulation, Modelling and Simulation Society of Australia and New Zealand, 1596–1602.
4. Abd El-Kawy, O. R., Rød, J. K., Ismail, H. A. and Suliman, A. S., 2011. Land use and land cover change detection in the western Nile delta of Egypt using remote sensing data, Applied Geography, 31(2), 483–494. https://doi.org/10.1016/j.apgeog.2010.10.012.
5. Ahmadzadeh, H., Morid, S., Delavar, M. and Srinivasan, R., 2016. Using the SWAT model to assess the impacts of changing irrigation from surface to pressurized systems on water productivity and water saving in the Zarrineh Rud catchment, Agricultural Water Management, 175, 15–28. https://doi.org/10.1016/j.agwat.2015.10.026.
6. Bailey, R. T., Wible, T. C., Arabi, M., Records, R. M. and Ditty, J., 2016. Assessing regional-scale spatio-temporal patterns of groundwater–surface water interactions using a coupled SWAT-MODFLOW model, Hydrological Processes, 30(23), 4420–4433. https://doi.org/10.1002/hyp.10933.
7. Baker, T. J. and Miller, S. N., 2013. Using the Soil and Water Assessment Tool (SWAT) to assess land use impact on water resources in an East African watershed, Journal of Hydrology, 486, 100–111. https://doi.org/10.1016/j.jhydrol.2013.01.041.
8. Beven, K. and Binley, A., 1992. The future of distributed models: Model calibration and uncertainty prediction, Hydrological Processes, 6(3), 279–298. https://doi.org/10.1002/hyp.3360060305.
9. Coppin, P., Jonckheere, I., Nackaerts, K., Muys, B. and Lambin, E., 2004. Digital Change Detection Methods in Ecosystem Monitoring: A Review, International Journal of Remote Sensing, 25, 1565–1596. https://doi.org/10.1080/0143116031000101675.
10. Coulter, L. L., Stow, D. A., Tsai, Y. H., Ibanez, N., chien Shih, H., Kerr, A., Benza, M., Weeks, J. R. and Mensah, F., 2016. Classification and assessment of land cover and land use change in southern

Ghana using dense stacks of Landsat 7 ETM+ imagery, Remote Sensing of Environment, 184, 396–409. https://doi.org/10.1016/j.rse.2016.07.016.

11. Dariane, A. and Eamen, L., 2017. Finding the Causes and Evaluating Their Impacts on Urmia Lake Crisis Using a Comprehensive Water Resources Simulation Model, JHS, 3(2), 62-77. https://doi.org/10.22055/JHS.2018.24762.1064
12. Devolent, T. M., Lepczyk, C. A., Chen, Q., Miura, T. and Cox, L. J., 2017. Assessing multi-decadal land-cover – land-use change in two wildlife protected areas in Tanzania using Landsat imagery, PLoS ONE, 12(9), 1–20. https://doi.org/10.1371/journal.pone.0185468.
13. Dowlatabadi, S. and Zomorodian, S. M. A., 2016. Conjunctive simulation of surface water and groundwater using SWAT and MODFLOW in Firoozabad watershed, KSCE Journal of Civil Engineering, 20(1), 485–496. https://doi.org/10.1007/s12205-015-0354-8
14. Du, J., Rui, H., Zuo, T., Li, Q., Zheng, D., Chen, A., Xu, Y. and Xu, C. Y., 2013. Hydrological Simulation by SWAT Model with Fixed and Varied Parameterization Approaches Under Land Use Change, Water Resources Management, 27(8), 2823–2838. https://doi.org/10.1007/s11269-013-0317-0.
15. Eamen, L. and Alireza B. Dariane, 2014. Agricultural Development Role in Urmia Lake Crisis, Iran, Tech4Dev International Conference, UNESCO Chair in Technologies for Development: What is Essential?, 4-6 June, EPFL, Lausanne, Switzerland.
16. Eimanifar, A. and Mohebbi, F., 2007. Urmia Lake (Northwest Iran): A brief review, Saline Systems, 3(1). https://doi.org/10.1186/1746-1448-3-5.
17. Fathian, F., Dehghan, Z. and Eslamian, S., 2016. Evaluating the impact of changes in land cover and climate variability on streamflow trends (case study: Eastern subbasins of Lake Urmia, Iran), International Journal of Hydrology Science and Technology, 6(1), 1–26. https://doi.org/10.1504/IJHST.2016.073881.
18. Fohrer, N., Haverkamp, S., Eckhardt, K. and Frede, H. G., 2001. Hydrologic response to land use changes on the catchment scale, Physics and Chemistry of the Earth, Part B: Hydrology, Oceans and Atmosphere, 26(7–8), 577–582. https://doi.org/10.1016/S1464-1909(01)00052-1.
19. Gashaw, T., Tulu, T., Argaw, M., Worqlul, A. W., Tolessa, T. and Kindu, M., 2018. Estimating the impacts of land use/land cover changes on Ecosystem Service Values: The case of the Andassa watershed in the Upper Blue Nile basin of Ethiopia, Ecosystem Services, 31, 219–228. https://doi.org/10.1016/j.ecoser.2018.05.001.
20. Ghaffari, G., Keesstra, S., Ghodousi, J. and Ahmadi, H., 2010. SWAT-simulated hydrological impact of land-use change in the Zanjanrood Basin, Northwest Iran, Hydrological Processes, 24(7), 892–903. https://doi.org/10.1002/hyp.7530.
21. van Griensven, A. and Meixner, T., 2006. Methods to quantify and identify the sources of uncertainty for river basin water quality models, Water Science and Technology, 53(1), 51–59. https://doi.org/10.2166/wst.2006.007.
22. Gross, D., 2005. Monitoring Agricultural Biomass Using NDVI Time Series, Food and Agriculture Organization of the United Nations (FAO), Rome, Italy.

23. Hassanzadeh, E., Zarghami, M. and Hassanzadeh, Y., 2012. Determining the Main Factors in Declining the Urmia Lake Level by Using System Dynamics Modeling, Water Resources Management, 26(1), 129–145. https://doi.org/10.1007/s11269-011-9909-8.
24. Islam, K., Jashimuddin, M., Nath, B. and Nath, T. K., 2018. Land use classification and change detection by using multi-temporal remotely sensed imagery: The case of Chunati wildlife sanctuary, Bangladesh, Egyptian Journal of Remote Sensing and Space Science, 21(1), 37–47. https://doi.org/10.1016/j.ejrs.2016.12.005.
25. Kennedy, J. and Eberhart, R., 1995. Particle Swarm Optimization, International Conference on Neural Networks, Western Australia, Australia. https://doi.org/10.1109/ICNN.1995.488968.
26. Kim, N. W., Chung, I. M., Won, Y. S. and Arnold, J. G., 2008. Development and application of the integrated SWAT-MODFLOW model, Journal of Hydrology, 356(1–2), 1–16. https://doi.org/10.1016/j.jhydrol.2008.02.024.
27. Kuczera, G. and Parent, E., 1998. Monte Carlo assessment of parameter uncertainty in conceptual catchment models: The Metropolis algorithm, Journal of Hydrology, 211(1–4), 69–85. https://doi.org/10.1016/S0022-1694(98)00198-X.
28. Leavesley, G. H., Lichty, R. W., Troutman, B. M., Saindon, L. G., 1984. Precipitation-runoff Modeling System: User's Manual, U.S. Geological Survey Water resources, Investigation Report 83-4238.
29. Lunetta, R. S., Knight, J. F., Ediriwickrema, J., Lyon, J. G. and Worthy, L. D., 2006. Land-cover change detection using multi-temporal MODIS NDVI data, Remote Sensing of Environment, 105(2), 142–154. https://doi.org/10.1016/j.rse.2006.06.018.
30. Moore, I. D., Grayson, R. B. and Ladson, A. R., 1991. Digital terrain modelling: A review of hydrological, geomorphological, and biological applications, Hydrological Processes, 5(1), 3–30. https://doi.org/10.1002/hyp.3360050103.
31. Muttitanon, W. and Tripathi, N. K., 2005. Land use/land cover changes in the coastal zone of Ban Don Bay, Thailand using Landsat 5 TM data, International Journal of Remote Sensing, 26(11), 2311–2323. https://doi.org/10.1080/01431160512331326666.
32. Neitsch, S. L., Arnold, J. G., Kiniry, J. R. and Williams, J. R., 2011. Soil & Water Assessment Tool Theoretical Documentation Version 2009, Texas Water Resources Institute.
33. Nelson, R. F., 1983. Detecting Forest Canopy Change Due to Insect Activity Using 3 Landsat MSS, Photogrammetric Engineering and Remote Sensing.
34. Owojori, A. and Xie, H., 2005. Landsat Image-Based LULC Changes of San Antonio, Texas Using Advanced Atmospheric Correction and Object-Oriented Image Analysis Approaches, 5th International Symposium on Remote Sensing of Urban Areas, 14-16 March, Tempe, USA.
35. Quyen, N. T. N., Liem, N. D. and Loi, N. K., 2014. Effect of land use change on water discharge in Srepok watershed, Central Highland, Viet Nam, International Soil and Water Conservation Research, 2(3), 74–86. https://doi.org/10.1016/S2095-6339(15)30025-3.
36. Schilling, K. E. and Libra, R. D., 2003. Increased baseflow in Iowa over the second half of the 20th Century, Journal of the American Water Resources Association, 39(4), 851–860.

https://doi.org/10.1111/j.1752-1688.2003.tb04410.x.

37. Schulz, S., Darehshouri, S., Hassanzadeh, E., Tajrishy, M. and Schüth, C., 2020. Climate change or irrigated agriculture – what drives the water level decline of Lake Urmia, Scientific Reports, 10(1), 1–10. https://doi.org/10.1038/s41598-019-57150-y.
38. Singh, A., 1989. Review Articlel Digital change detection techniques using remotely-sensed data, International Journal of Remote Sensing, 10(6), 989–1003. https://doi.org/10.1080/01431168908903939.
39. Thanapakpawin, P., Richey, J., Thomas, D., Rodda, S., Campbell, B. and Logsdon, M., 2007. Effects of landuse change on the hydrologic regime of the Mae Chaem river basin, NW Thailand, Journal of Hydrology, 334(1–2), 215–230. https://doi.org/10.1016/j.jhydrol.2006.10.012.
40. Wigmosta, M. S., Vail, L. W. and Lettenmaier, D. P., 1994. A distributed hydrology-vegetation model for complex terrain, Water Resources Research, 30(6), 1665–1679. https://doi.org/10.1029/94WR00436.
41. Xiao, J., Shen, Y., Ge, J., Tateishi, R., Tang, C., Liang, Y. and Huang, Z., 2006. Evaluating urban expansion and land use change in Shijiazhuang, China, by using GIS and remote sensing, Landscape and Urban Planning, 75(1–2), 69–80. https://doi.org/10.1016/j.landurbplan.2004.12.005.
42. Xie, Y., Sha, Z. and Yu, M., 2008. Remote sensing imagery in vegetation mapping: a review, Journal of Plant Ecology, 1(1), 9–23. https://doi.org/10.1093/jpe/rtm005.
43. Zurqani, H. A., Post, C. J., Mikhailova, E. A., Schlautman, M. A. and Sharp, J. L., 2018. Geospatial analysis of land use change in the Savannah River Basin using Google Earth Engine, International Journal of Applied Earth Observation and Geoinformation, 69(March), 175–185. https://doi.org/10.1016/j.jag.2017.12.006.

Figures

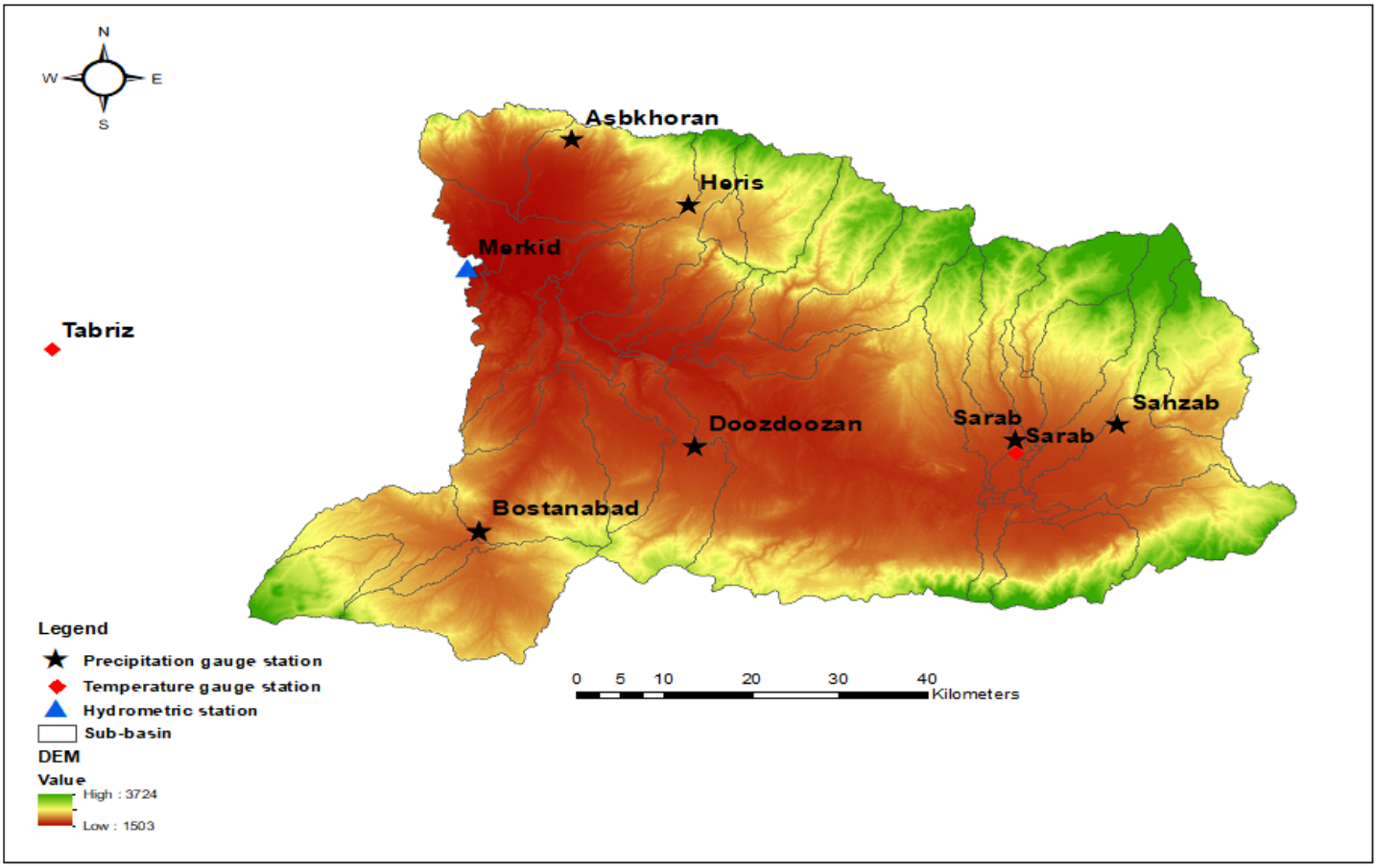

Figure 1

Dispersion of precipitation, temperature, and hydrometric stations Note: The designations employed and the presentation of the material on this map do not imply the expression of any opinion whatsoever on the part of Research Square concerning the legal status of any country, territory, city or area or of its authorities, or concerning the delimitation of its frontiers or boundaries. This map has been provided by the authors.

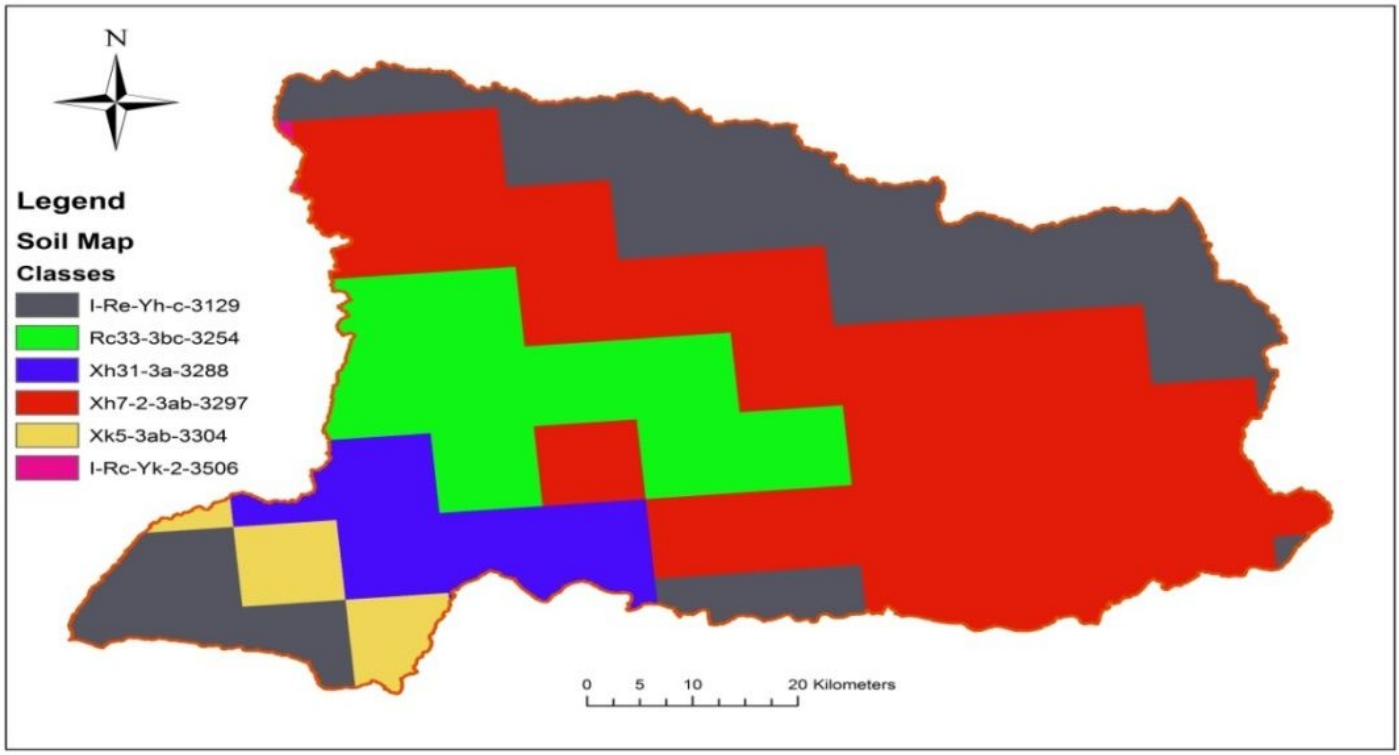

Figure 2

Soil map of the case study Note: The designations employed and the presentation of the material on this map do not imply the expression of any opinion whatsoever on the part of Research Square concerning the legal status of any country, territory, city or area or of its authorities, or concerning the delimitation of its frontiers or boundaries. This map has been provided by the authors.

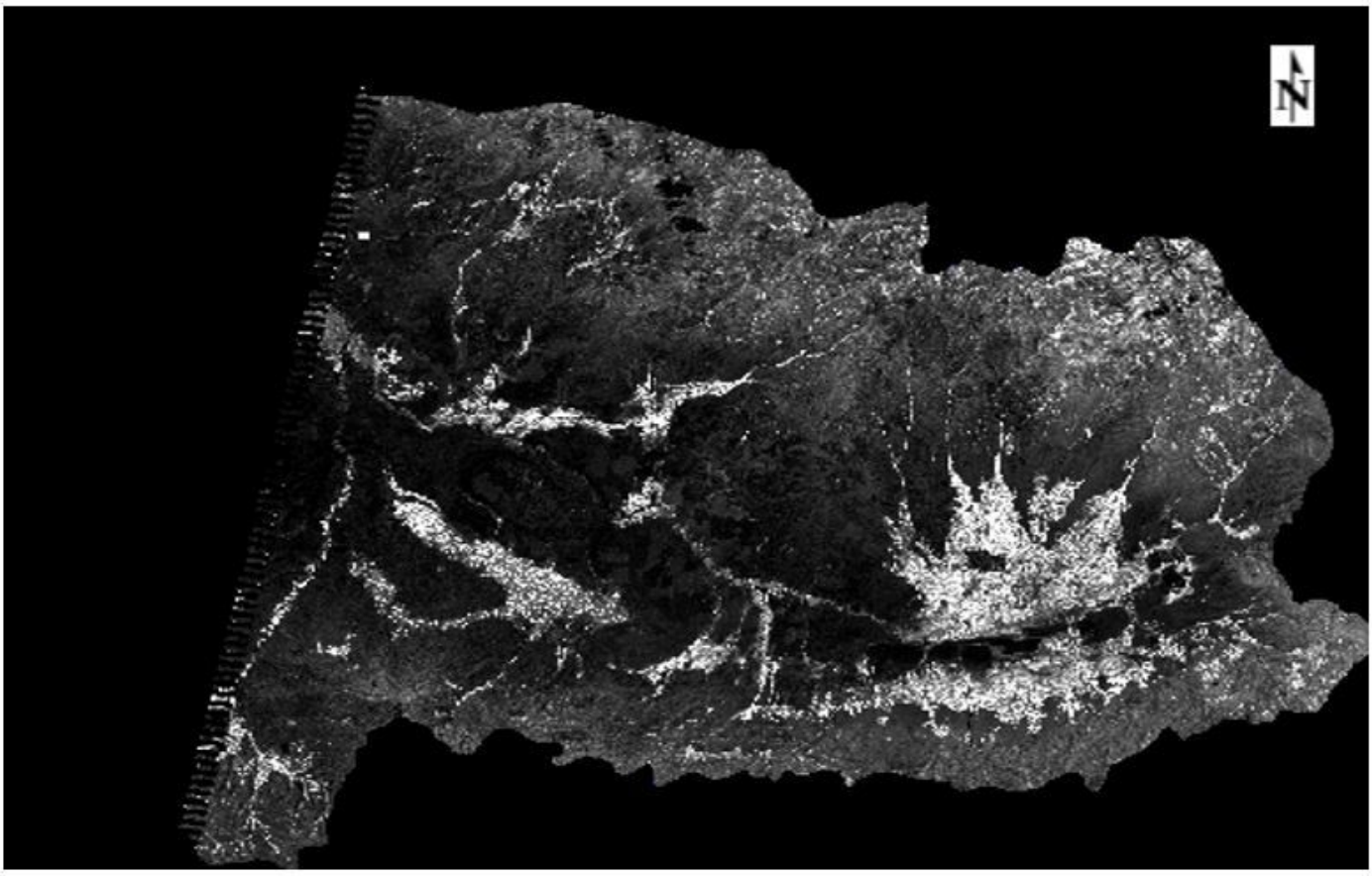

Figure 3

NDVI image of the case study. Note: The designations employed and the presentation of the material on this map do not imply the expression of any opinion whatsoever on the part of Research Square concerning the legal status of any country, territory, city or area or of its authorities, or concerning the delimitation of its frontiers or boundaries. This map has been provided by the authors.

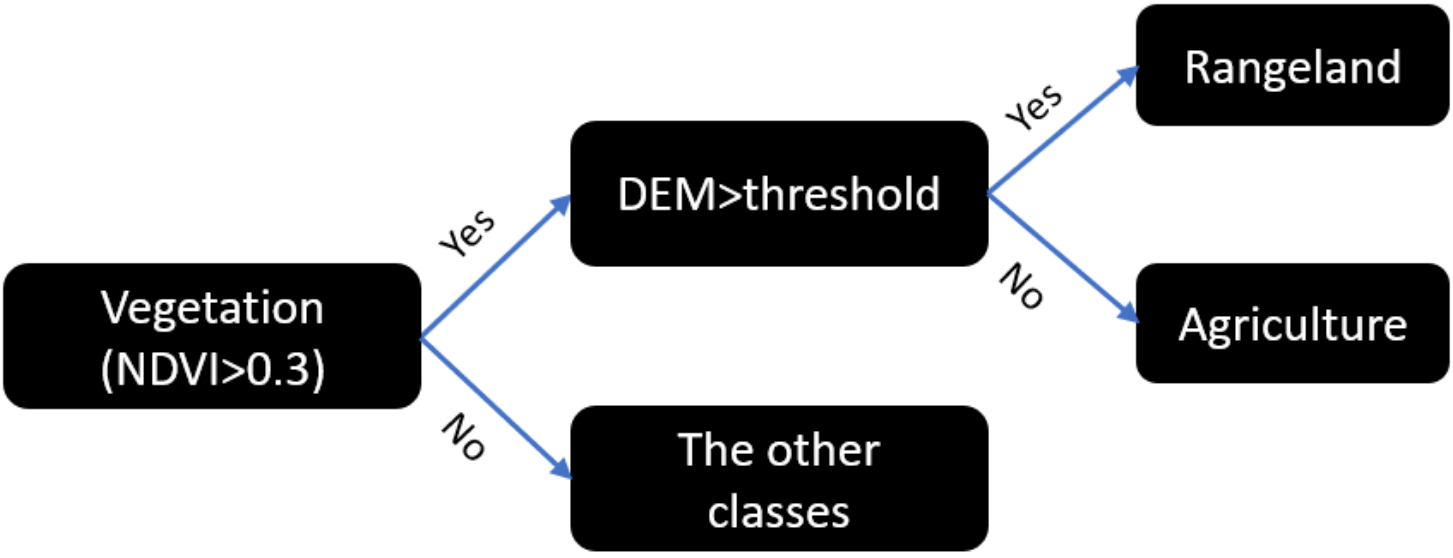

Figure 4

Decision tree to divide the vegetation class into agriculture and rangeland classes

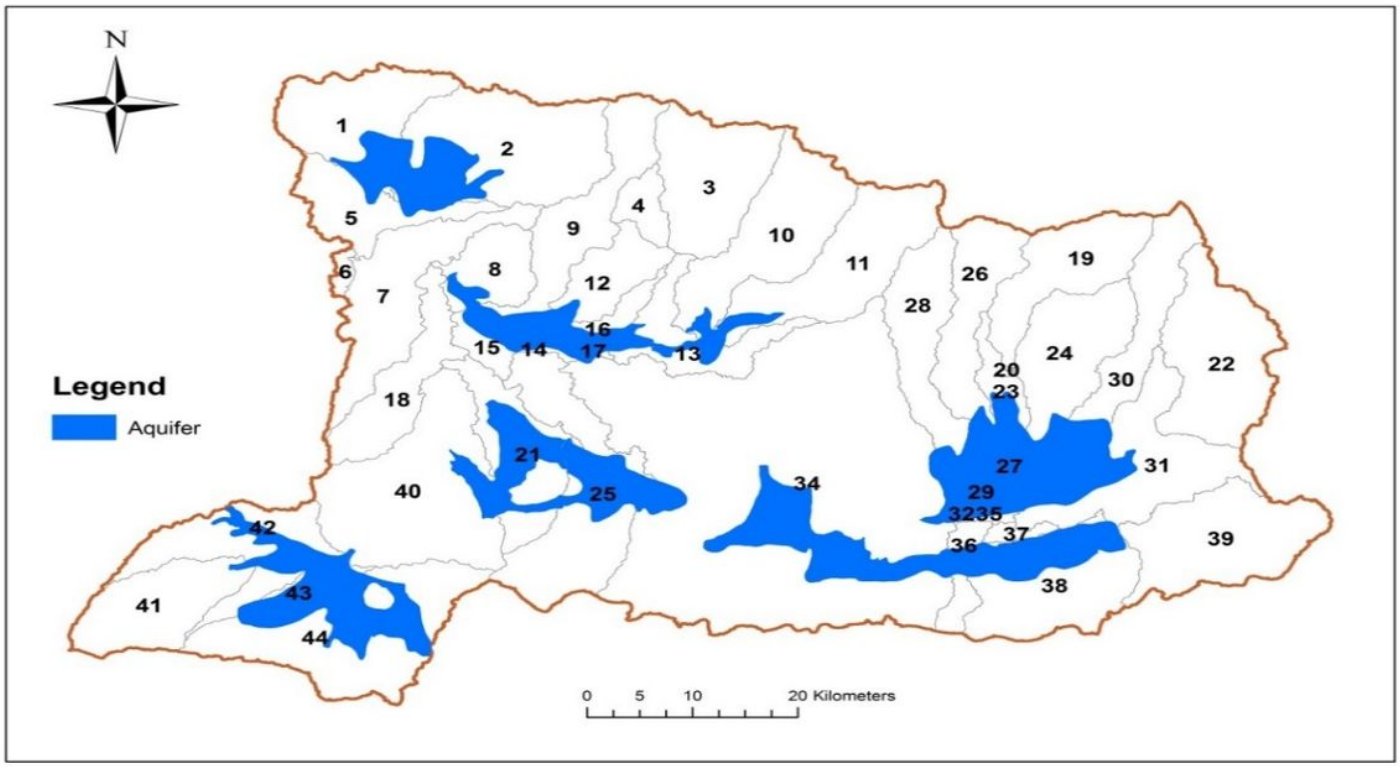

Figure 5

The basin's aquifer map pictured on the modeled basin Note: The designations employed and the presentation of the material on this map do not imply the expression of any opinion whatsoever on the part of Research Square concerning the legal status of any country, territory, city or area or of its authorities, or concerning the delimitation of its frontiers or boundaries. This map has been provided by the authors.

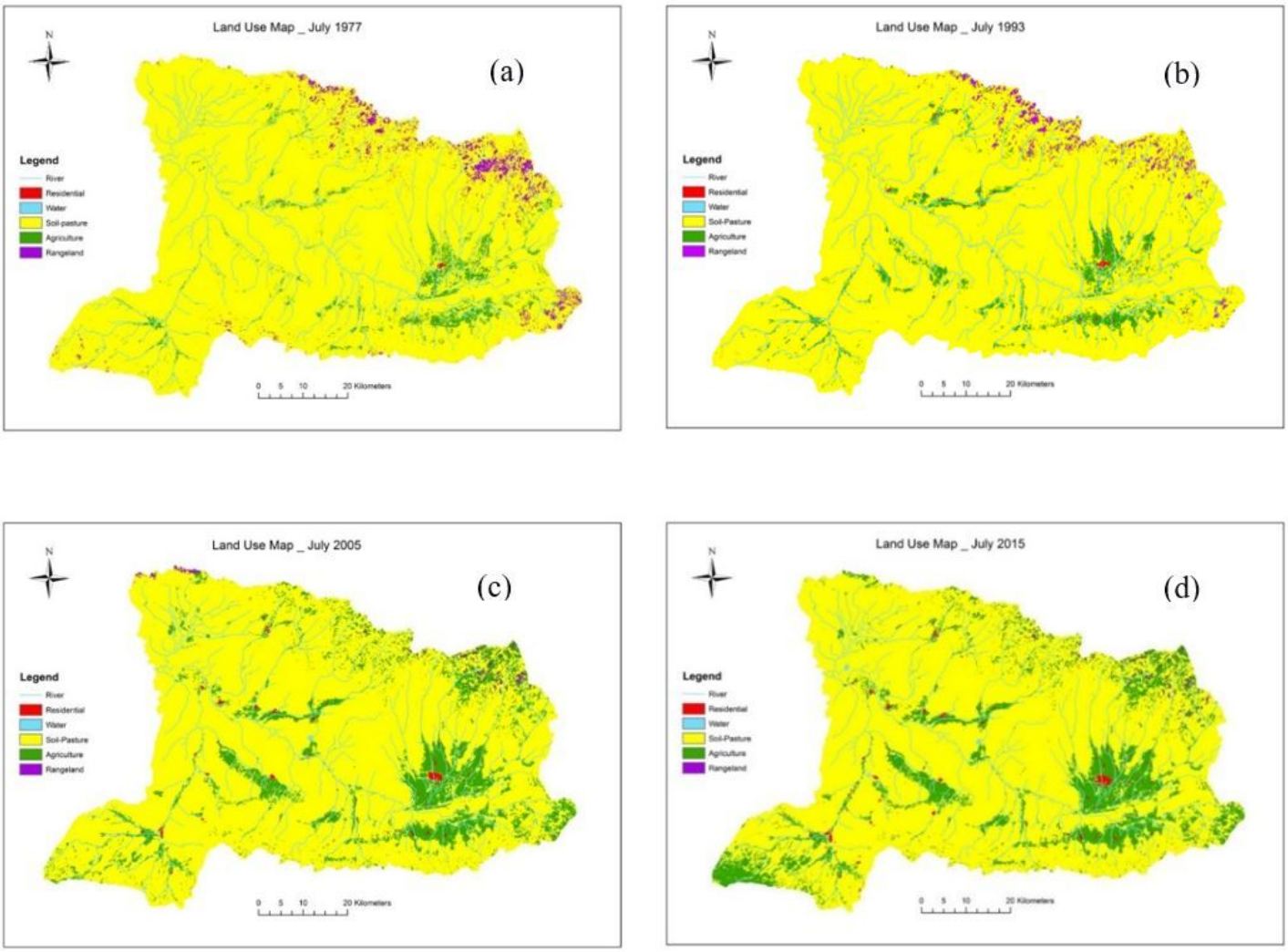

Figure 6

Generated land-use maps for July (a) 1977 (b) 1993 (c) 2005 and (d) 2015 Note: The designations employed and the presentation of the material on this map do not imply the expression of any opinion whatsoever on the part of Research Square concerning the legal status of any country, territory, city or area or of its authorities, or concerning the delimitation of its frontiers or boundaries. This map has been provided by the authors.

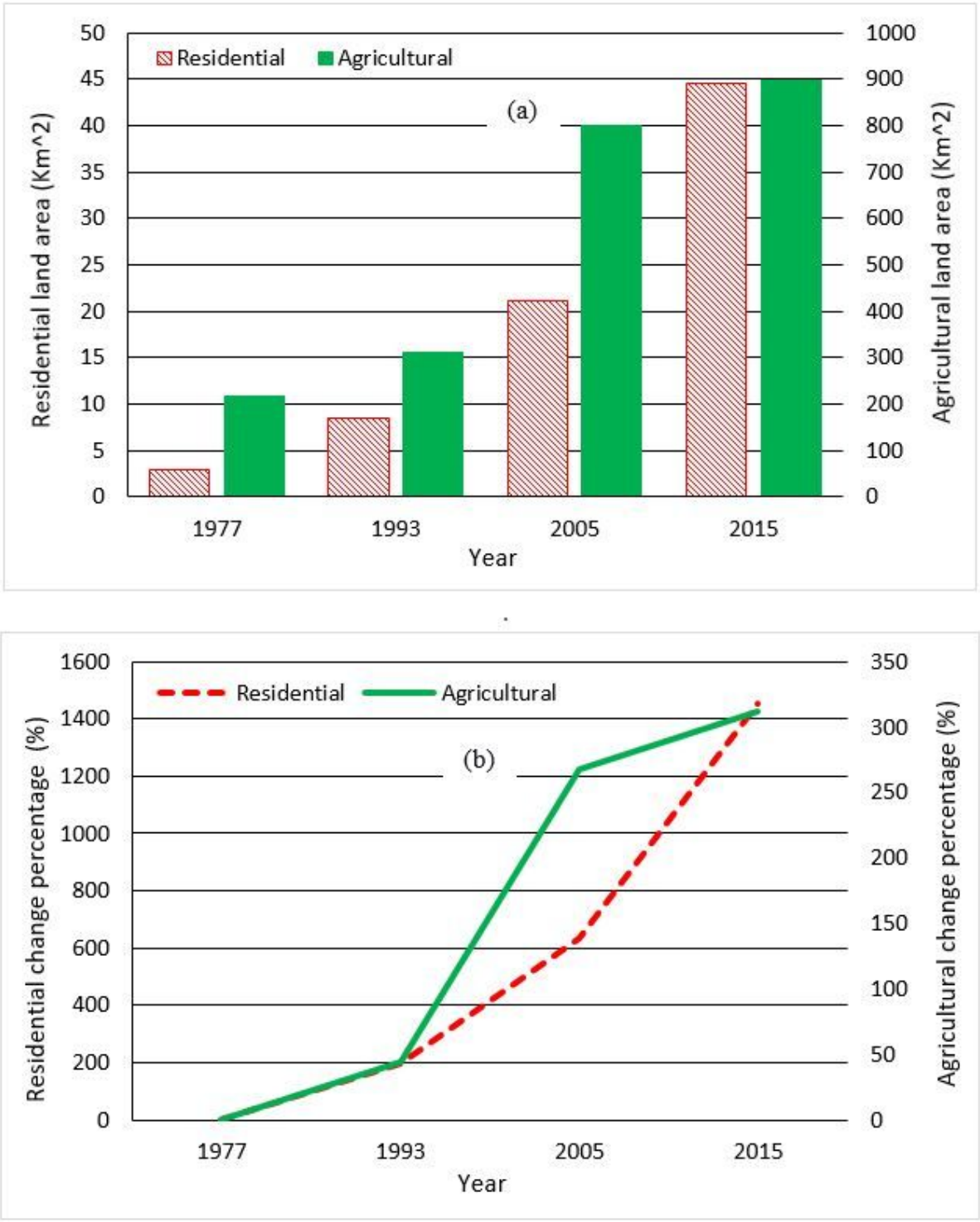

Figure 7

Agricultural and residential classes for selected years (a) land areas and (b) change percentage

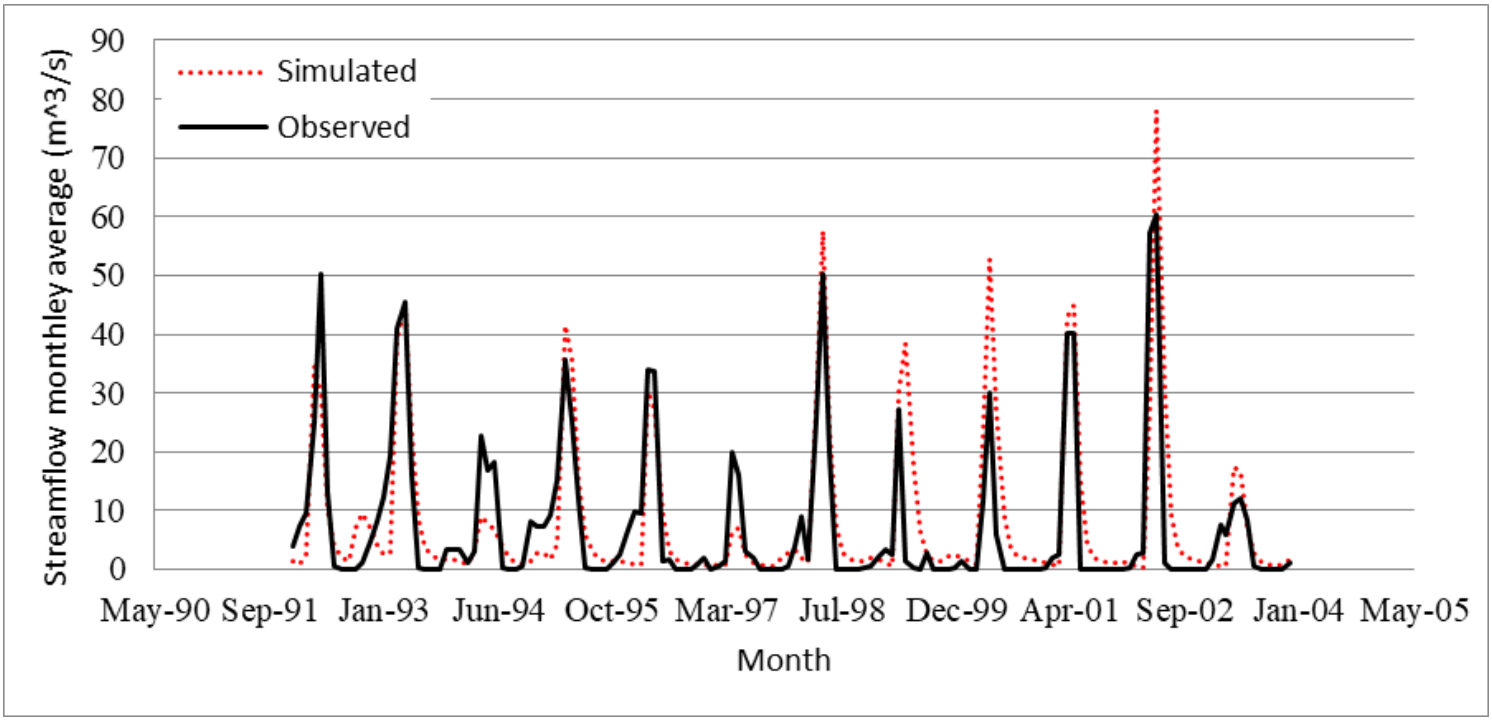

Figure 8

Monthly average of the simulated and observed streamflow for the calibration and validation periods

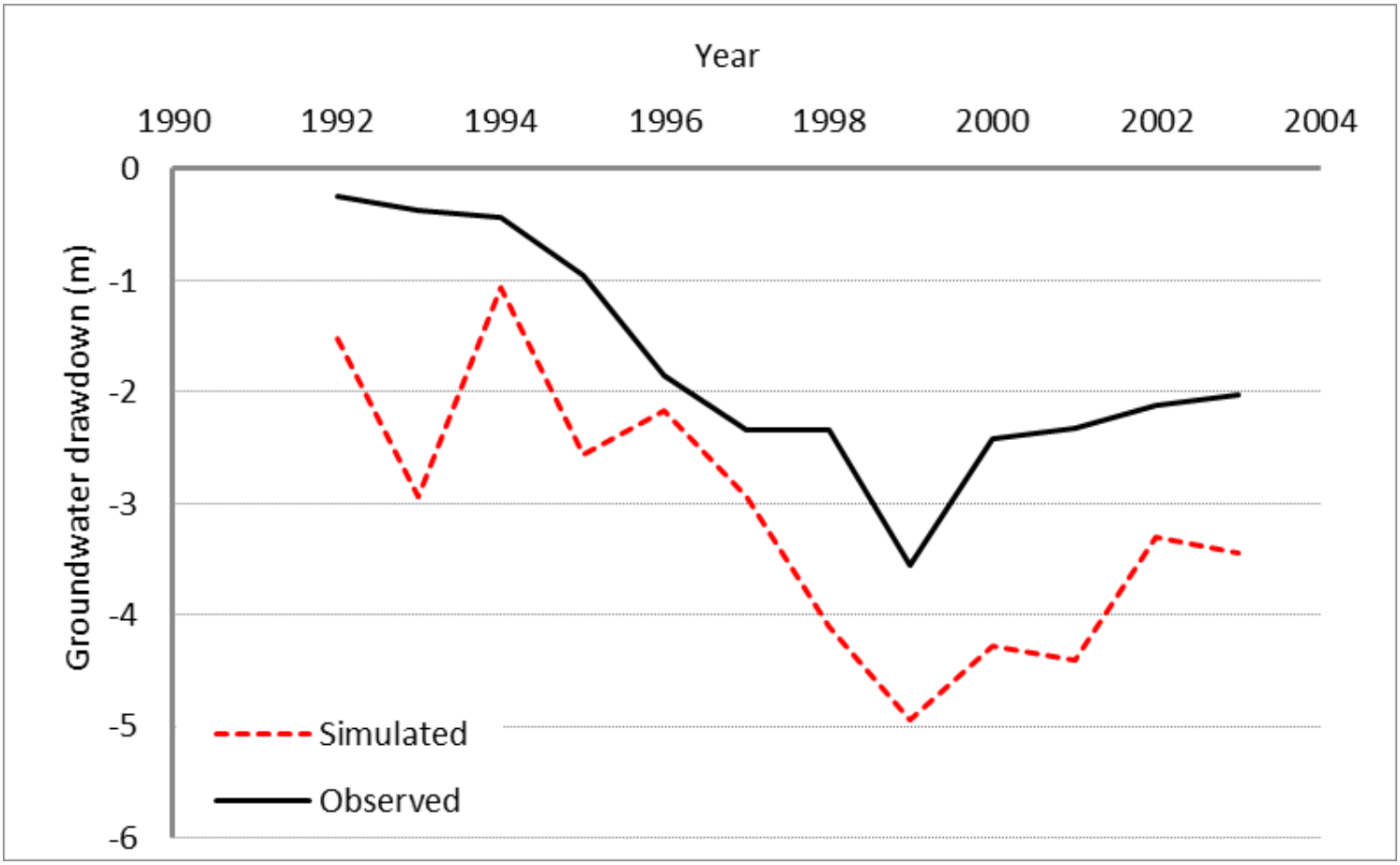

Figure 9

Comparison of simulated groundwater drawdown to the observation values, Sarab plain.

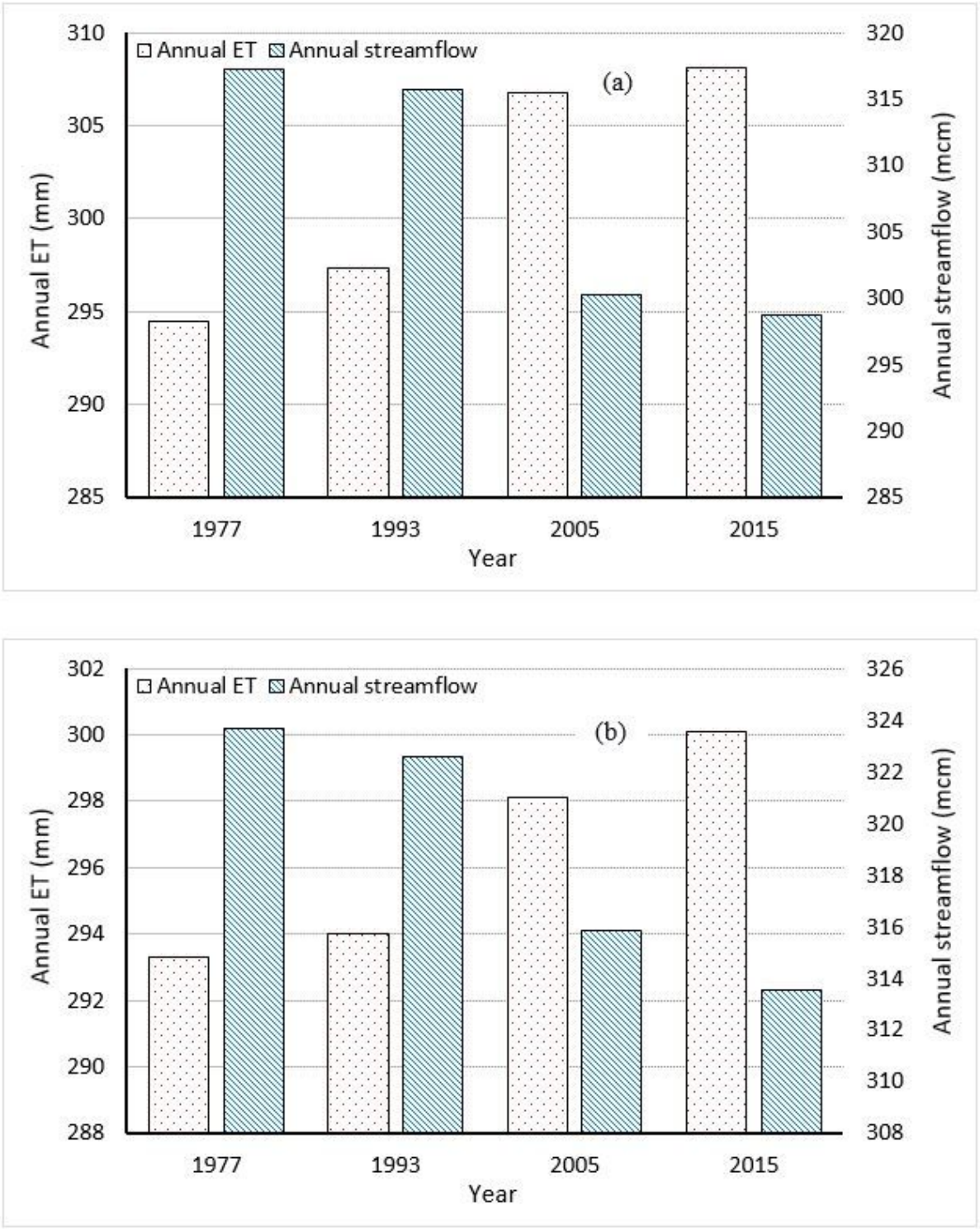

Figure 10

Average annual ET and streamflow for (a) irrigation scenario and (b) no-irrigation scenario

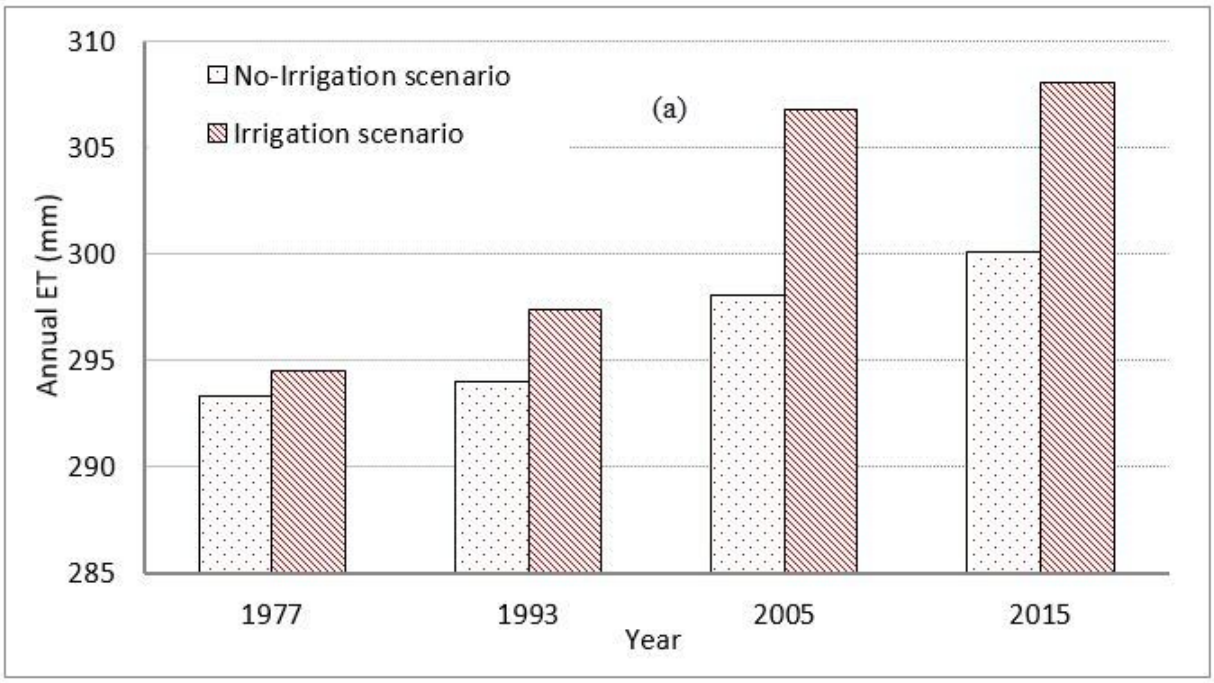

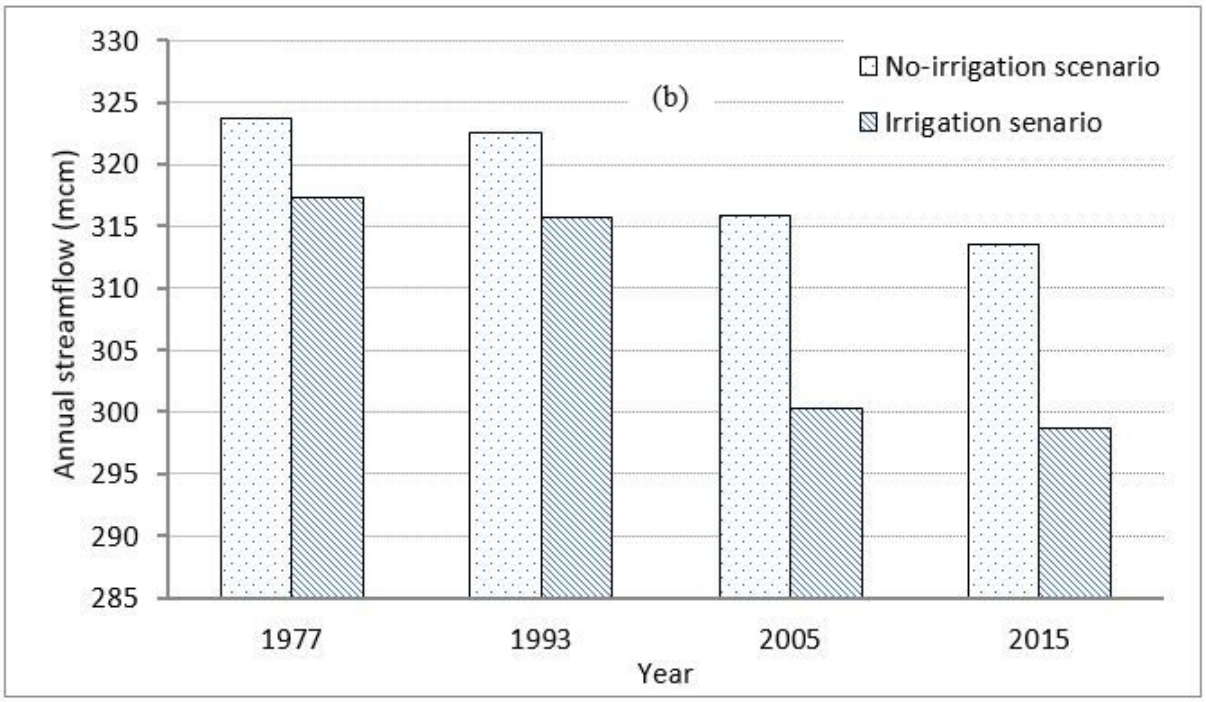

Figure 11

Comparison of (a) annual average ET and (b) annual average streamflow for irrigation and no-irrigation scenarios